

# Earth's Future

## RESEARCH ARTICLE

10.1029/2024EF005130

# Statistical Distribution of Urban Area Reveals a Converging Trend of Global Urban Land Expansion



### Key Points:

- Area distributions of global urban systems evolve along the direction away from an initial power law toward an exponential distribution
- Urban area distribution shift can be attributed to the increasing influence of external economies of scale associated with globalization
- Urban area distribution shift lead to reduced stability and resilience of urban systems and increased health risks for urban dwellers

Shengjie Hu<sup>1,2</sup> , Zhenlei Yang<sup>3</sup> , Sergio Andres Galindo Torres<sup>1,2</sup> , Zipeng Wang<sup>4</sup>, Haoying Han<sup>5,6</sup>, Yoshihide Wada<sup>7,8</sup> , Thomas Cherico Wanger<sup>1,2,9</sup>, and Ling Li<sup>1,2</sup> 

<sup>1</sup>School of Engineering, Westlake University, Hangzhou, China, <sup>2</sup>Key Laboratory of Coastal Environment and Resources of Zhejiang Province, Westlake University, Hangzhou, China, <sup>3</sup>State Key Laboratory of Desert and Oasis Ecology, Key Laboratory of Ecological Safety and Sustainable Development in Arid Lands, Xinjiang Institute of Ecology and Geography, Chinese Academy of Sciences, Urumqi, China, <sup>4</sup>School of Science, Westlake University, Hangzhou, China, <sup>5</sup>Center for Balance Architecture, Zhejiang University, Hangzhou, China, <sup>6</sup>Innovation and Design, City University of Macau, Macau, China, <sup>7</sup>Climate and Livability, Center for Desert Agriculture, Biological and Environmental Science and Engineering Division, King Abdullah University of Science and Technology, Thuwal, Saudi Arabia, <sup>8</sup>Biodiversity and Natural Resources Program, International Institute for Applied Systems Analysis (IIASA), Laxenburg, Austria, <sup>9</sup>Agroecology, Department of Crop Sciences, University of Göttingen, Göttingen, Germany

### Supporting Information:

Supporting Information may be found in the online version of this article.

### Correspondence to:

T. C. Wanger and L. Li,  
tomcwanger@westlake.edu.cn;  
liling@westlake.edu.cn

### Citation:

Hu, S., Yang, Z., Galindo Torres, S. A., Wang, Z., Han, H., Wada, Y., et al. (2025). Statistical distribution of urban area reveals a converging trend of global urban land expansion. *Earth's Future*, 13, e2024EF005130. <https://doi.org/10.1029/2024EF005130>

Received 17 JUL 2024

Accepted 4 DEC 2024

**Abstract** Urban land expansion is a major driver of many environmental and societal changes that challenge human well-being and sustainable development, but its evolutionary process and dynamics are neither clear nor well-integrated into urban science quantitatively. We analyzed the global urban extent data based on nighttime lights to examine the statistical distribution of urban land area at the global scale, and in 13 regions and countries over 29 years. The results reveal a converging temporal trend in urban land expansion from subnational to global scales, characterized by a coherent shift of urban area distribution from an initial power law toward an exponential distribution. This trend is well captured by a unified mathematical model based on the shifted power law distribution function and is reflected in the gradual predominance of medium-size cities over small-size cities in the configuration of urban systems across the world. The shift of urban area distributions bears the consequence of reduced urban system stability and resilience, and can be linked to increasing exposure of urban populations to extreme heat events and air pollution. These changes are likely to be driven by the increasing influence of external economies of scale associated with globalization. The findings challenge the status quo of land urbanization practices and emphasize the importance of medium-size cities in urban planning.

**Plain Language Summary** The rapid growth of urban land has become a major environmental concern and sustainability challenge, but its growth pattern and dynamics are not fully understood. Based on global urban extent data from 1992 to 2020, we quantified the evolutionary process of urban land expansion in 14 regions and countries by analyzing the statistical distribution of urban land area, and further explored its impacts on the functioning of urban systems and their inhabitants by introducing methods from statistical physics. For the first time, we show a coherent temporal shift away from initial power law to exponential distributions of urban land area across all the investigated spatial scales. This trend can be described by a unified mathematical model and can be attributed to the increasing influence of external economies of scale associated with globalization. During this evolutionary process, urban systems become less stable and resilient, and urban residents are exposed to increased risks from the urban heat island effect and PM2.5 pollution. These results call for a rethinking of current ways of how land is urbanized in order to ensure a sustainable future for humanity.

## 1. Introduction

One of the most defining changes that humanity has brought about since the Industrial Revolution is the rapid replacement of natural land with urban structures to support growing urban populations (Ouyang et al., 2022; Solecki et al., 2013). Urban land growth indeed facilitated socio-economic development and improved human living conditions, sometimes summarized as urban economies of scale (Batty, 2013; Bettencourt & West, 2010). However, it also brings with it social inequality (He et al., 2022), environmental degradation (Liang & Yang, 2019), biodiversity decline (Laurance & Engert, 2022) and direct threats to human health, such as the urban heat island effect (UHI) and fine particulate matter (PM2.5) pollution (Southerland et al., 2022; Tuholse et al., 2021). For current environmental and sustainability issues, how human societies use and manage land is

© 2024. The Author(s).

This is an open access article under the terms of the [Creative Commons Attribution-NonCommercial-NoDerivs License](#), which permits use and distribution in any medium, provided the original work is properly cited, the use is non-commercial and no modifications or adaptations are made.

both a source of problems and solutions (Meyfroidt et al., 2022); therefore, understanding the trajectory of how land is urbanized (or simply land urbanization) is critical to ensuring a sustainable future for humanity (Acuto et al., 2018).

Urban land expansion has long been a concern and many studies have been conducted previously. The global urban land area was found to have tripled over the past 30 years, with an increasing trend in the annual share of global urban land in Asia, while a decreasing and a stable trend in Europe and North America, respectively (Zhao et al., 2021). The urban land use per capita has been shown to increase over time, but the population density of urban expansion may remain constant, increase or decrease in different regions, influenced by the effects of economy, consumer preferences for proximity, etc (Angel, 2023). These previous studies have examined the growth patterns of urban land mainly in terms of quantity, speed and population density, and explained regional differences based on theories from geography and urban economics. Since Jacobs (1961) referred to cities as “organized complexity”, the study of cities as complex systems has emerged as a new frontier in urban science. In the study of complex systems, probability distributions are often taken as the first quantitative characteristic of the system to detect possible regularities (Sornette, 2007). The mathematical forms of the distributions can provide constraints and guidelines to identify the underlying mechanism at their origin, and to indicate the state and function of the system, thus shedding light on the system's behavior and dynamics (Chen et al., 2018; Sornette, 2007). Therefore, the size distribution of the ensemble of cities (i.e., the urban system) as well as its spatio-temporal variations has been considered as the key to revealing the fundamental laws and dynamics of urban systems (Barthelemy, 2019; Batty, 2013; Bettencourt, 2013). The statistical lens of urban studies has mainly focused on population size, showing different distribution functions, including Zipf's law (power law), log-normal and q-exponential, for population data from different countries or regions, with opposite temporal trends, that is, approaching the power law distribution in some countries while moving away from it in others (Arshad et al., 2018; Bettencourt & Zünd, 2020). Urban land area is another important proxy for city size, representing the physical space of cities, but its statistical distribution has received less attention, let alone its evolutionary characteristics and dynamics (Rozenfeld et al., 2011). An essential property of complex systems that the whole is more than the sum of its parts suggests that the connections between their statistics, state and function, and underlying driving mechanisms cannot be captured by conventional individual-based methods and require holistic, systematic approaches (Holovatch et al., 2017; Sornette, 2007). Statistical physics, with its focus on explaining and predicting measurable properties and behaviors of macroscopic systems, provides theories and methods that can address the above challenges of studying complex systems (Barthelemy, 2019; Fan et al., 2021). Hence, depicting the trajectory of land urbanization from a statistical perspective using methods from statistical physics has the potential to bring new understanding to the patterns and dynamics of urban land expansion. On the other hand, cities emerge from the aggregation of people, which is generically driven by economies of scale composed of internal and external parts (Batty, 2013; Bettencourt & West, 2010; Brenner & Schmid, 2015). Globalization, another defining feature of our time, has strengthened the interconnectedness, interdependence and integration among cities, resulting in an increased influence from external economies of scale at the city level (Brady et al., 2007; Young et al., 2006). However, how urban systems in regions with different political, economic and demographic conditions respond to this driving force change remains unknown, especially in the land dimension. Moreover, while it is recognized that urban land growth poses health risks to urban dwellers, the specific relationship between the two needs to be further explored (Seto & Fragkias, 2005). As a result, despite extensive research, the patterns, particularly in statistical terms, of urban land growth across regions, its impacts on urban systems and urban dwellers, and how such patterns are formed are not fully understood.

To fill the above knowledge gaps, we analyzed the statistical distribution of urban land area and its changes from 1992 to 2020 in 14 regions covering global, continental, national and subnational scales. From this system-level analysis, we identified a coherent shift in urban area distribution among different urban systems, which can be described by a unified evolutionary equation based on the shifted power law distribution. The urban area distribution shift was then linked to alterations of system state (e.g., heterogeneity and orderliness) and function (e.g., stability and resilience) using fluctuation, entropy and power spectrum analyses to account for its impact on urban systems. We explained the evolutionary characteristics of urban systems through the changing role of internal and external economies of scale. The implications of our findings for current land urbanization practices were discussed by linking urban system changes to altered exposure of urban populations to extreme heat and PM2.5 pollution.

## 2. Study Area and Materials

### 2.1. Study Area

This study was carried out in 14 countries and regions, including the globe, continents other than Antarctica, the United States of America (USA), China, India and the four economic zones of China (Figure S1 in Supporting Information S1). These regions were chosen to cover (a) various spatial scales, from local to global, considering that the urbanization process unfolds on multiple scales (Solecki et al., 2013); (b) diverse political, economic, social and cultural backgrounds, as the practice of land urbanization is influenced by these aspects (Solecki et al., 2013); and (c) different stages of urbanization, as exemplified by the counter-urbanization and re-urbanization process undergone by developed regions like Europe and USA, and the rapid urbanization process experienced by developing regions such as Africa and China (Mao et al., 2008); thereby revealing common features and patterns of urban land expansion with general implications for urban researchers and policy makers in different regions.

### 2.2. Definitions and Data

How to define cities and their areas is still a matter of debate in urban studies (Angel, 2023; Batty & Ferguson, 2011; Dong et al., 2024). Existing approaches to delineate the spatial extent of cities include those based on administrative boundaries, population size or density (Angel, 2023; Rozenfeld et al., 2011), functional urban area (Bettencourt, 2021), built environment (Potere et al., 2009), nighttime lights (Zhao et al., 2021) and cell-phone data (Dong et al., 2024). These delineations emphasize different aspects of city size, each with its own advantages and limitations, as extensively argued in previous studies (Dong et al., 2024; Shi et al., 2023), and how a city is defined should depend on the context and scope of the study. Because urban regions are brightly lit at the night, they can be identified in nighttime light remote sensing data (Levin et al., 2020). Although it is from the perspective of human activities agglomeration rather than administration, nighttime light data has the advantage of mapping urban land expansion with global coverage and long temporal periods, which gives it the potential to measure spatio-temporal changes in socioeconomic activities and urbanization processes (Levin et al., 2020; Rozenfeld et al., 2011). Therefore, we used a global data set of annual urban extents from 1992 to 2020 with 1 km resolution based on nighttime lights (Zhao et al., 2021) to quantify the evolutionary process of urban land growth. The cities discussed here are entities with spatial extents associated with intensive human settlements and high-intensity socioeconomic activities, rather than cities in the commonly used administrative sense, and the urban system refers to the ensemble of cities within the study region.

The global data set of annual urban extents we used was developed based on the harmonized time-series nighttime light imagery facilitated by data of water masks, global artificial impervious area and etc. in a stepwise-partitioning framework integrating multiple algorithms by Zhao et al. (2021). It has been cross-evaluated with other global urban products, historical google maps and socioeconomic statistics, and shown to be reliable (Zhao et al., 2021). Nonetheless, nighttime light data may be affected by national or local energy efficiency or other control policies. Such effects are difficult to quantify, but are relatively small and can be neglected in our long-term analysis. The long-term urban land data set was established for each study region with the assistance of ArcGIS 10.2.

The currently available classification of city size is mainly based on population. According to the World Cities Report (U.N. Habitat, 2022), cities can be divided into four types: small cities ( $50,000 \leq \text{population} < 250,000$ ), medium-sized cities ( $250,000 \leq \text{population} < 1,000,000$ ), large cities ( $1,000,000 \leq \text{population} < 5,000,000$ ) and very large cities ( $\text{population} \geq 5,000,000$ ). Since the population density ranges from 1,700 to 15,000 (people/km<sup>2</sup>) worldwide, the extent of urban areas for each of the above city types can be determined as small cities (3.3–16.7 km<sup>2</sup>), medium-sized cities (16.7–66.7 km<sup>2</sup>), large cities (66.7–333.3 km<sup>2</sup>) and very large cities (>333.3 km<sup>2</sup>). According to these results and the urban data used, we also defined four types of city based on urban land area ( $A$ ), that is, small-size cities ( $A < 10^1$  km<sup>2</sup>), medium-size cities ( $10^1 \leq A < 10^2$  km<sup>2</sup>), large-size cities ( $10^2 \leq A < 10^3$  km<sup>2</sup>) and mega-size cities ( $A \geq 10^3$  km<sup>2</sup>).

Economies of scale, recognized as one of the main drivers of the emergence of cities, refer here to the benefits obtained by a city when the urban area increases, and its internal and external parts are the benefits brought by the urban land growth inside and outside the city, respectively. In practice, it is difficult to isolate and quantify these two parts because they are intertwined and influenced by many factors. However, as the interconnectedness and

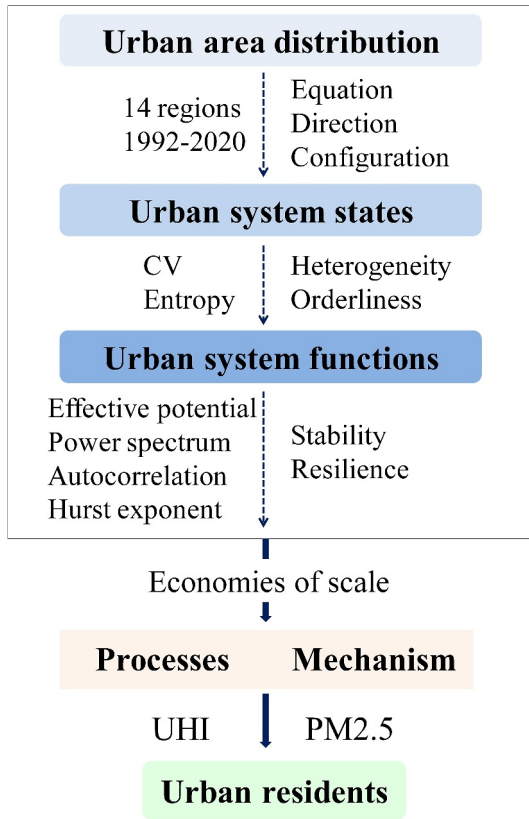


**Figure 1.** The research framework established for studying urban systems at the system level.

interdependence between regions has been strengthened by globalization (Brady et al., 2007; Gu, 2019; Young et al., 2006), the globalization index (GI), which measures the globalization degree of a region, can to some extent represent the degree to which a region is influenced by external economies of scale. The KOF Globalization Index data was used because it comprehensively considers the economic, social and political dimensions of globalization, and has a long time span from 1970 to 2019 (Gygli et al., 2019). As this is a country-level data set, the GI data for each continent were calculated as the average of all countries on that continent.

The impacts of urban system changes on urban dwellers were analyzed in terms of UHI and PM2.5 pollution based on data sets of Global High Resolution Daily Extreme Urban Heat Exposure (UHE-Daily, 1983–2016; Tuholske et al., 2021) and The Annual PM2.5 Concentrations for Countries and Urban Areas (1998–2016; CIESIN, 2021), respectively. These two hazards were analyzed because they are closely associated with urban land expansion and are among the leading contributors to the global burden of disease (Southerland et al., 2022; Tuholske et al., 2021), and their data coverage is consistent with the urban extent data set. By spatially overlaying the UHE-Daily with the boundaries of the 14 study regions, the total annual exposure of urban population within each region was determined. Based on the city types we defined and the PM2.5 data, the average PM2.5 concentrations were calculated for each city type using area as a weight. Due to the limited sample size of these two data sets, these analyses were performed at global, continental and national scales.

### 3. Methodology

To study the patterns and dynamics of urban land expansion across regions, we established a systematic approach with the following framework

(Figure 1): (a) determining the probability distribution of urban area and its evolution trend to characterize the growth pattern of urban land; (b) quantifying the corresponding changes of urban system state in terms of heterogeneity and orderliness using coefficient of variation and information entropy; (c) quantifying the corresponding changes of urban system function in terms of stability and resilience through effective potential and power spectrum analysis; (d) investigating the driving mechanism underlying the above changes of urban systems based on economies of scale; and (e) analyzing the impacts of urban land growth patterns on urban residents in terms of UHI and PM2.5.

#### 3.1. Determination of the Probability Distribution of Urban Land Area

The shifted power law distribution (Equation 1a) was proposed by Mandelbrot (1953) by adding a shift coefficient ( $b \geq 0$ ) to the power law distribution. This distribution exhibits different behavior as the value of  $b$  increases, that is, it reduces to a power function at  $b = 0$  (Equation 1b) and can be approximated by the exponential (Equation 1c) and uniform distribution (Equation 1d) as  $b$  approaches positive infinity.

$$f(x) = C(x + b)^{-\alpha} \quad (a > 1; b \geq 0; C > 0) \quad (1a)$$

$$\text{if } b = 0, f(x) \propto x^{-\alpha} \quad (1b)$$

$$\text{if } b \rightarrow +\infty, \alpha \rightarrow +\infty, \text{ and } \frac{\alpha}{b} = r, f(x) \propto e^{-rx} (r > 0) \quad (1c)$$

$$\text{if } b \rightarrow +\infty, f(x) \approx \frac{1}{x_{max} - x_{min}} \quad (x_{max} > x_{min} > 0) \quad (1d)$$

where  $x$  is the variable of interest within  $[x_{min}, x_{max}]$ ;  $f(x)$  denotes the probability density function (PDF) of  $x$ ;  $\alpha$ ,  $b$  and  $C$  are the coefficients of  $f(x)$  called the scaling exponent, shift coefficient and proportion term, respectively;

and  $r$  is a constant number. For more information on the definition of the shifted power law distribution and the derivation of its limit behavior, see Text S1 in Supporting Information S1.

The shifted power law distribution was fitted to the urban land area data in each study region in the form of the complementary cumulative density function (CCDF, Equation 2b). The CCDF was used instead of the PDF (Equation 2a) because it is more robust against the fluctuations caused by finite system size (Newman, 2005). The fitted coefficients of urban area distributions vary among regions but all increase over time, with the temporal variation of the shift coefficient ( $b$ ) following exponential functions in most regions (Equation 2c), while the scaling exponent ( $a$ ) and the proportion term ( $c$ ) were related to  $b$  by linear and quadratic functions, respectively (Equations 2d and 2e).

$$p(A) = \Pr(X = A) = C(A + b)^{-\alpha} \quad (\alpha > 1; b \geq 0; C > 0) \quad (2a)$$

$$P(A) = \Pr(X \geq A) = c(A + b)^{-a} \quad (a = \alpha - 1 > 0; c > 0) \quad (2b)$$

$$b(t) = c_1 e^{c_1' t} \quad (t = Year - 1992) \quad (2c)$$

$$a(b) = c_2 + c_2' b \quad (2d)$$

$$c(b) = c_3 + c_3' b + c_3'' b^2 \quad (2e)$$

where  $A$  represents the urban land area ( $A \in [A_{min}, A_{max}]$ ) with the unit of  $\text{km}^2$ , which is the statistical variable we are interested in;  $X$  is the observed value of  $A$ ;  $p(A)$  and  $P(A)$  are the PDF and CCDF of  $A$ , respectively, and the latter is the urban area distribution we are studying;  $\alpha$  and  $a$  are the scaling exponents of the PDF and CCDF for  $A$ , respectively, and  $a$  ranges from 0 to 2 according to the fitting results;  $b$  denotes the shift coefficient;  $t$  is the time index, starting from zero (i.e., year of 1992);  $C$  and  $c$  represent the proportion terms which are constrained by the full probability condition;  $c_1, c_1', c_2, c_2', c_3, c_3'$  and  $c_3''$  are fitting parameters.

All fittings in this paper were performed through the `scipy.optimize.curve_fit` model in Python 3 (<https://www.python.org/>) and the fit performance was assessed by the coefficient of determination ( $r^2$ ) and root mean squared error (RMSE). See Text S2 in Supporting Information S1 for details.

### 3.2. Quantification of Urban System State

#### 3.2.1. Heterogeneity and Orderliness

The coefficient of variation (CV, Equation 3) and the information entropy (H, Equation 4) are two measures commonly used in statistical physics to describe the state of a system. CV can reflect the degree of heterogeneity of a system, that is, the larger the CV value, the higher the degree of heterogeneity (Loreau & De Mazancourt, 2013). H quantifies the degree of chaos of the system state and a higher value of H indicates a more chaotic system state (Michaelides, 2008).

$$CV = \frac{\sigma}{\mu} \quad (3)$$

$$H = -\sum_{i=1} p_i(A) \log_2 p_i(A) \quad (4)$$

where  $\sigma$  and  $\mu$  are the standard deviation and mean of the urban area ( $A$ ) of an urban land data set, respectively; and  $p_i(A)$  represents the probability of the  $i$ -th urban area in the whole data set.

#### 3.2.2. Phase Separation

To illustrate the relationship between the change in urban system state and the change in its probability distribution, we further analyzed the urban area distribution of each region and observed two coexisting components, that is, a flat “shoulder” at the lower limit and a power law-like “body” at the upper limit. By comparing the shifted power law distribution and the power law distribution with the same coefficients (Equations 5a–5c), we found that when the urban areas are large, the effect of  $b$  can be neglected and the distribution approximately

follows a power law; otherwise, the influence of  $b$  is evident, causing urban areas smaller than  $b$  to deviate from the power law. Thus, the  $b$  value can be used as the critical area to separate the two components. The annual urban land data in each region were then divided into two subsets: the shoulder subset, consisting of the cities with areas smaller than  $b$ , and the body subset, containing all remaining cities, with sample sizes denoted as  $N_1$  and  $N_2$ , respectively. The shoulder subset was found to fit well the stretched-exponential distribution (Equation 6), while the body subset conforms to the power law distribution (Equation 7). Analogous to the concepts of state and phase in statistical physics (Zaccone, 2020), we refer to these two distributions as the two phases of urban system state. The balance and competition of the two phases in the area distribution can be quantified by calculating the proportions of cities locating in each component, denoted as  $R_1$  (stretched-exponential phase, Equation 8a) and  $R_2$  (power law phase, Equation 8b), respectively.

$$y_1(A) = \log[c(A + b)^{-a}] = \log(c) - a \log(A + b) \quad (5a)$$

$$y_2(A) = \log(cA^{-a}) = \log(c) - a \log(A) \quad (5b)$$

$$\Delta y(A) = |y_1(A) - y_2(A)| = \left| a \log\left(\frac{1}{1 + b/A}\right) \right| \quad (5c)$$

$$P_{se}(A) = \Pr(X \geq A) = C_1 A^{\epsilon-1} e^{-C_1' A^\epsilon} \quad (A_{min} \leq A < b; \epsilon < 0) \quad (6)$$

$$P_{pl}(A) = \Pr(X \geq A) = C_2 A^{-a_{pl}} \quad (b \leq A \leq A_{max}; a_{pl} > 0) \quad (7)$$

$$R_1 = \frac{N_1}{N_1 + N_2} \quad (8a)$$

$$R_2 = \frac{N_2}{N_1 + N_2} \quad (8b)$$

Where  $y_1(A)$  and  $y_2(A)$  are log-transformed CCDF functions corresponding to the shifted power law and the power law distribution of the urban area ( $A$ ), respectively, and  $\Delta y(A)$  denotes the difference between them;  $P_{se}(A)$  and  $P_{pl}(A)$  denote the stretched-exponential and the power law distribution of the urban area ( $A$ ), respectively;  $X$  is the observed value of  $A$ ;  $\epsilon$  represents the exponent of the stretched-exponential distribution;  $a_{pl}$  is the power exponent of the power law distribution with values between 0 and 2, depending on the results of the fit;  $C_1$ ,  $C_1'$ , and  $C_2$  are fitting parameters.

### 3.3. Quantification of Urban System Function

#### 3.3.1. Stability

The effective potential (EP) is a measure of the macrostate stability of a system by means of its PDF and the most likely state of the system is the one with the minimum value of EP (Martín et al., 2015). Following the definition of EP (Equation 9), the PDF of the urban area ( $p(A)$ ), Equation 2a) was used to derive the EP of the urban system. The result showed that the EP value of the urban system is positively related to  $b$ , indicating that the stability of the urban system will decrease as the value of  $b$  increases.

$$EP = -\log(p(A)) = a \log(A + b) - \log(C) \quad (9)$$

where  $p(A)$  is the PDF of the urban area ( $A$ );  $\alpha$ ,  $b$  and  $C$  are the function coefficients, the same as in Equation 2a.

#### 3.3.2. Resilience

According to the critical tipping theory, if the system loses its resilience (i.e., the ability of the system to maintain its current state or functions in the face of perturbations; Pascual & Guichard, 2005), it would take longer for the system to return to its pre-perturbation state, leading to an increase in autocorrelation within the system (Scheffer

et al., 2009). Thus, the alterations in system resilience can be detected by its autocorrelation function, which is the Fourier counterpart of the system's power spectrum and can be derived from its probability distribution.

The area power spectrum,  $S(\varphi)$ , corresponding to the power law phase (Equation 7) of the urban area distribution was established through the transformation used in Bak et al. (1987), given below,

$$S(\varphi) = \int_b^{A_{max}} \frac{A p_{pl}(A)}{1 + (\varphi A)^2} dA \propto \varphi^\gamma \quad (\gamma = a_{pl} - 1) \quad (10)$$

where  $A$  is the urban area of the power law phase ( $A \in [b, A_{max}]$ );  $\varphi$  represents the transformed quantity corresponding to  $A$ ;  $p_{pl}(A)$  denotes the PDF corresponding to the power law phase of the urban area distribution;  $a_{pl}$  is the power exponent of the power law phase; and  $\gamma$  is the exponent of the power spectrum. The value of spectrum exponent  $\gamma$  indicates the type of power spectrum (Halley, 1996). If  $\gamma = 0$ , the power spectrum is a white noise type; if  $\gamma < 0$ , it is classified as the pink noise; if  $\gamma > 0$ , it belongs to the blue noise. A detailed derivation of the area power spectrum and more information on these “colored” noises can be found in Text S3 and Text S4, respectively.

The autocorrelation function ( $R(\tau)$ ), Equation 11a) can then be obtained by performing the Fourier transform on  $S(\varphi)$  (Kubo et al., 2012). When  $R(\tau)$  and  $S(\varphi)$  are assumed to be even functions, we can further derive the analytical expression of  $R(\tau)$  (Equation 11b) and analyze its behaviors under different types of  $S(\varphi)$ . The results showed that when  $S(\varphi)$  is a white noise ( $\gamma = 0$ ),  $R(\tau)$  is a  $\delta$  function (Equation 11c); when  $S(\varphi)$  belongs to pink noise ( $\gamma < 0$ ),  $R(\tau)$  asymptotically goes to zero (Equation 11d); and when  $S(\varphi)$  belongs to blue noise ( $\gamma > 0$ ),  $R(\tau)$  diverges, with a possibility of approaching infinity (Equation 11e). Therefore, the “blue shift” of urban area power spectrums, indicated by the spectrum exponent  $\gamma$  turning from negative to positive values, is likely to signify a decline of system resilience.

$$R(\tau) = \frac{1}{2\pi} \int_{-\infty}^{+\infty} S(\varphi) e^{i\varphi\tau} d\varphi \quad (11a)$$

$$\begin{aligned} R_A(\tau) &= \frac{1}{\pi} \int_0^{+\infty} \varphi^\gamma \cos \varphi\tau d\varphi \\ &= \frac{1}{\pi\tau} \varphi^\gamma \sin(\varphi\tau)|_{\varphi \rightarrow +\infty} + \frac{\gamma}{\pi\tau^2} \varphi^{\gamma-1} \cos(\varphi\tau)|_{\varphi \rightarrow +\infty} + \frac{\gamma(\gamma-1)}{\pi\tau^3} \varphi^{\gamma-2} \sin(\varphi\tau)|_{\varphi \rightarrow +\infty} \\ &\quad + \frac{\gamma(\gamma-1)(\gamma-2)}{\pi\tau^3} \int_0^{+\infty} \sin(\varphi\tau) \varphi^{\gamma-3} d\varphi \quad (-1 < \gamma < 1) \end{aligned} \quad (11b)$$

$$\text{if } \gamma = 0, R(\tau) = \frac{1}{\pi\tau} \sin(\varphi\tau)|_{\varphi \rightarrow +\infty} = \delta(\tau) \quad (11c)$$

$$\text{if } \gamma < 0, R(\tau)|_{\varphi \rightarrow +\infty} \rightarrow 0 \quad (11d)$$

$$\text{if } \gamma > 0, R(\tau) \approx \frac{1}{\pi\tau} \varphi^\gamma \sin(\varphi\tau)|_{\varphi \rightarrow +\infty} \text{ (diverge)} \quad (11e)$$

Since the  $S(\varphi)$  of all studied urban systems belongs to the fractional Gaussian noise ( $-1 < \gamma < 1$ ), their Hurst exponent ( $H_{urst}$ ) can be calculated using Equation 12 (Wornell, 1993). According to the fractional Brownian motion theory (Mandelbrot & Van Ness, 1968), the value of  $H_{urst}$  could reflect the coupling mode of the processes driving the changes of urban area growth and statistical distribution. To be specific,  $H_{urst} = 0.5$  indicates no correlation between processes,  $H_{urst} > 0.5$  indicates that the correlation between processes is persistent and  $H_{urst} < 0.5$  indicates that the correlation is anti-persistent (Mandelbrot & Van Ness, 1968).

$$H_{urst} = \frac{\gamma - 1}{2} + 1 \quad (12)$$

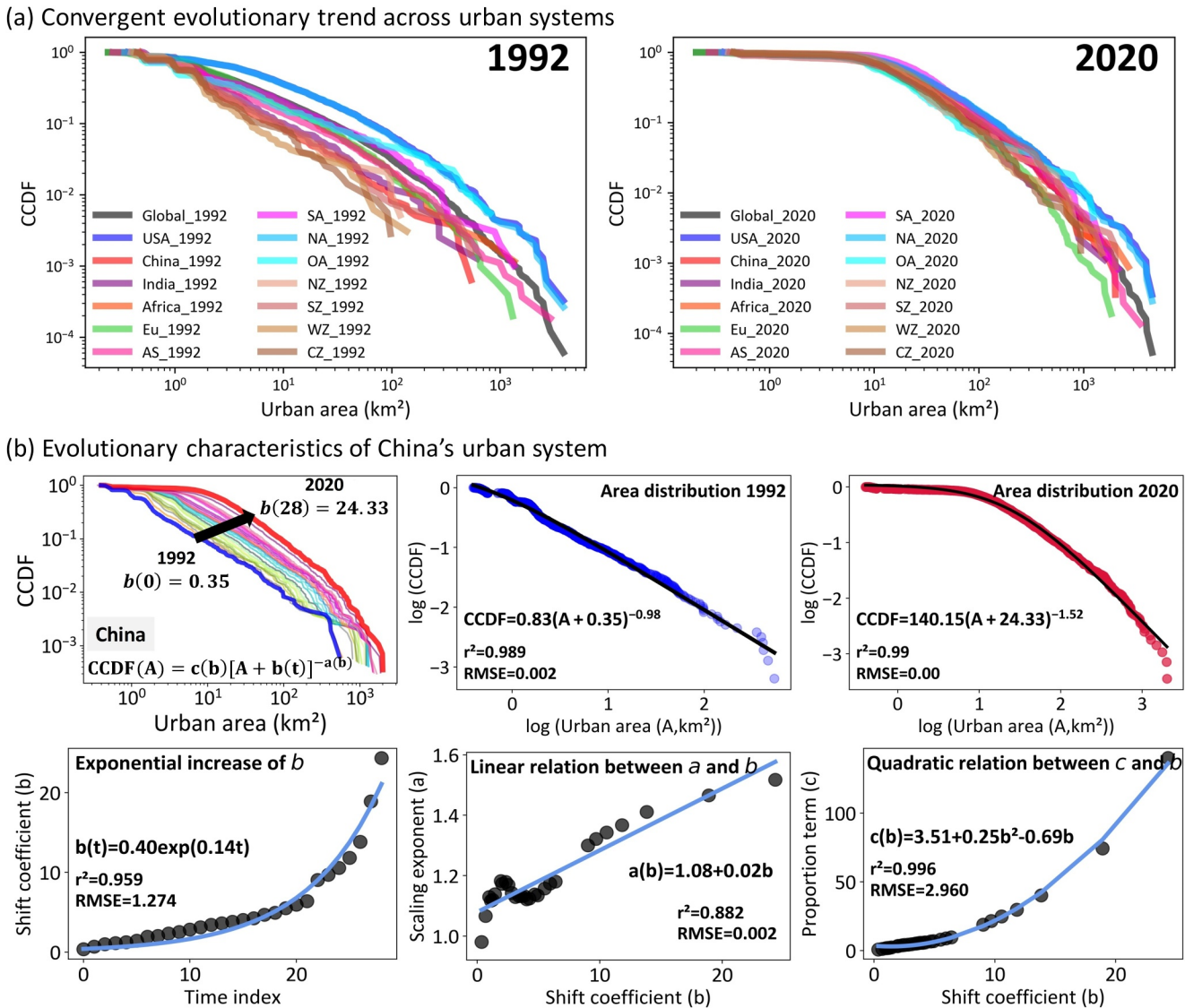


**Figure 2.** Evolution of the area distribution of urban systems. (a) The urban area distributions of the 14 study regions show a convergent evolutionary trend; (b) The evolutionary characteristics of a specific urban system, taking China as an illustrative example: the urban land areas obey the shifted power law distribution between 1992 and 2020, in which the shifted coefficient ( $b$ ) increases exponentially with time (here  $t = \text{Year}-1992$  is the time index), and the scaling exponent ( $a$ ) and the proportion term ( $c$ ) are linearly and quadratically related to  $b$ , respectively.

## 4. Results and Discussion

### 4.1. Convergent Evolution of Urban Area Distributions

Unlike previous studies based on changes in urban land area and population density, which showed different trends in urban land expansion across regions (Angel, 2023; Zhao et al., 2021), here we found that urban land areas in different regions follow the same distribution function, evolve along the same direction, undergo the same pattern shift in city configuration and exhibit a converging trend of changes across spatial scales and over time (Figure 1 and Movie S1). The urban area distributions of all 14 study regions well follow the shifted power law distribution from 1992 to 2020 (Figure 2b and Figures S2–S15 in Supporting Information S1). The three coefficients involved in the distribution function increases over time and are interrelated within each region, and such interrelationships can be described by the same functions in almost all regions (Figures 2b, 3a and 3b and Figures S16–S18 in Supporting Information S1). Specifically, the shift coefficient ( $b$ ) increases exponentially with time, which is particularly evident in developing regions (Figure 2b and Figure S16 in Supporting Information S1),



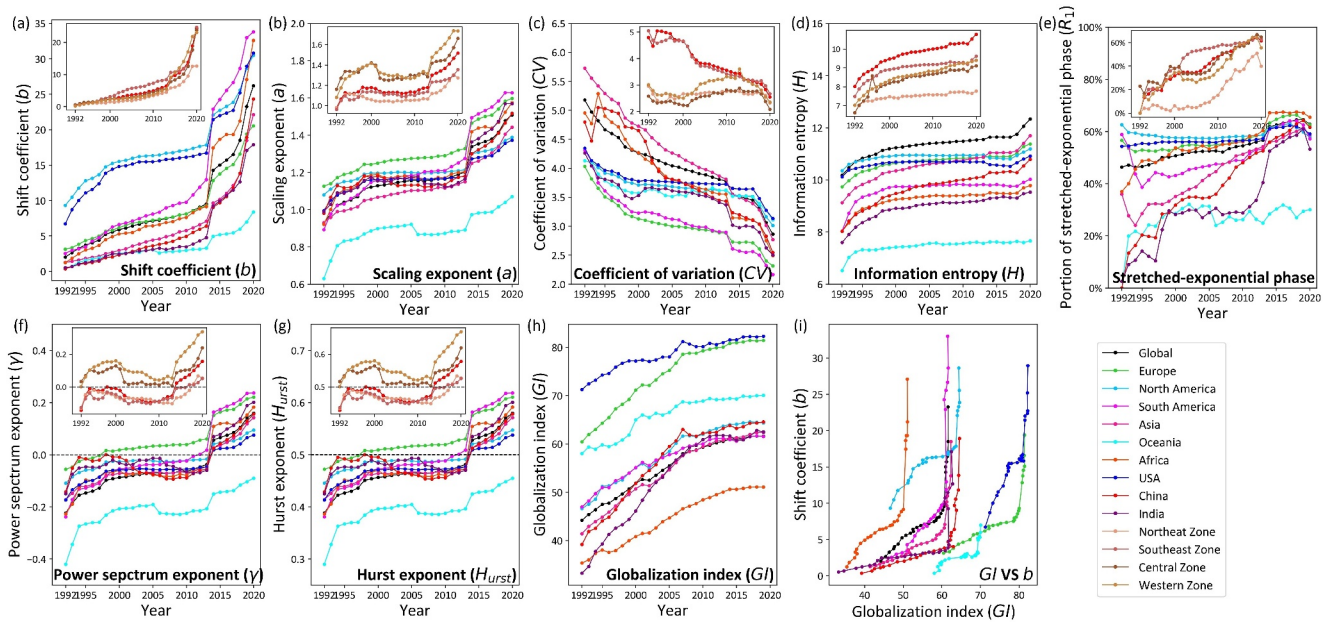


**Figure 3.** Temporal variations of indicators of urban system changes. (a)–(b) Coefficients of urban area distributions; (c)–(e) State indicators of urban systems; (f)–(g) Power spectrum variables; (h)–(i) Influence of external economies of scale. The enhanced influence from external economies of scale is represented by the increasing values of globalization index (GI) (h) and the positive correlations between GI values and the shifted coefficient ( $b$ ) values in all study regions (i). The subplots show the results for China and its four economic zones.

whereas the scaling exponent ( $a$ ) and the proportion term ( $c$ ) are linearly and quadratically related to  $b$ , respectively (Figure 2b and Figures S17–S18 in Supporting Information S1). Thus, the temporal evolution of urban area distributions can be recapitulated in a unified equation,  $P(A, t) = c(b)[A + b(t)]^{-a(b)}$  with  $b(t) \propto e^{c_1 t}$ . The exponential increase of  $b$  indicates that the urban area distribution evolves along the direction away from its initial power law distribution ( $b = 0$ ) at an accelerated rate and may approach the exponential or uniform distribution in the future. Since  $a$  and  $b$  are linearly correlated, the urban area distribution in all study regions is likely to enter the exponential regime first in the near future.

The corresponding changes in urban land arrangement were explored by analyzing the alterations in city configuration in terms of the proportional composition of different types of cities in a region. We found that the small-size cities dominated all regions at the beginning (1992), with higher proportions in developing regions like China (92%) than that in developed regions like USA (64%) (Table 1 and Table S2 in Supporting Information S1). Medium-size cities then gradually took the lead and accounted for around 60% worldwide by 2020. The portions of large- and mega-size cities also increased and showed their highest values (less than 1%) in North America (NA). These results demonstrated that the city configuration changes in the same manner and gradually becomes similar across regions, as evidenced by the collective shift of the dominant city type from small-to medium-size cities and the reduced regional disparities in the proportion of each type. The increase in the  $b$  value of the urban

**Table 1**  
Pattern Shift in the City Configuration Experienced by All Regions

Type	Global		EU		USA		China		China_SZ	
	1992	2020	1992	2020	1992	2020	1992	2020	1992	2020
Small	79.27%	29.80%	81.65%	37.28%	63.87%	20.79%	91.59%	29.30%	91.49%	33.83%
Medium	17.60%	60.24%	16.45%	55.64%	29.47%	65.11%	7.65%	61.81%	7.90%	55.57%
Large	2.98%	9.56%	1.86%	6.99%	6.24%	13.11%	0.76%	8.57%	0.61%	10.16%
Mega	0.15%	0.41%	0.04%	0.09%	0.42%	1.00%	0.00%	0.32%	0.00%	0.44%

*Note.* From small-size cities dominated to medium-size ones dominated. EU and SE are abbreviations for Europe and Southeast economic zone of China, respectively.

area distribution function corresponds to the increase in the proportion of medium-size cities in the city configuration.

## 4.2. Changes in the State and Function of Urban Systems

### 4.2.1. Reduced Heterogeneity and Orderliness in Urban System State

Coefficient of variation (CV) and information entropy (H), which respectively measure the degrees of heterogeneity and chaos of a system (Bowley & Sánchez, 1999; Michaelides, 2008), were calculated for each region. A trend of decreasing CV and increasing H emerges from all regions (Figures 3c and 3d), demonstrating that as urban area distributions deviated from their initial power law distributions, urban systems developed toward a relatively homogeneous and disordered state in the land dimension.

By further analyzing the distribution function of urban areas, we found a phase transition that is responsible for the change in system state. Specifically, the urban area distributions can be decomposed into two phases featured by stretched-exponential and power law distributions based on the values of  $b$  (Figure S19 in Supporting Information S1). A trend of expanding stretched-exponential phase and meanwhile contracting power law phase over time was observed in all study regions (Figure 3e and Figure S19 in Supporting Information S1). As shown by previous studies, the stretched-exponential distribution represents a homogeneous, disordered state (Hu et al., 2023), while the power law distribution indicates a heterogeneous, ordered state (Hu et al., 2023; Villegas et al., 2021). These results suggest that a phase transition, characterized by the expansion of the disordered phase and the contraction of the ordered phase, has occurred during the evolution of urban area distributions, driving the urban systems toward a homogeneous and disordered state. The increase of  $b$  value signals the state change of urban systems and indicates the degree of such change.

### 4.2.2. Reduced Stability and Resilience in Urban System Function

The decreasing trend in CV (Figure 3c) found in the urban area data also suggests that the size diversity (i.e., number of distinct urban areas) of urban systems has declined. Previous studies have shown that the size of a city affects how it responds to disturbances (Birkmann et al., 2016) and the decline in size diversity may result in a loss of response diversity that can destabilize the system (Elmqvist et al., 2003). Furthermore, it has been found that medium-size cities are more vulnerable to extreme events than mega cities (Birkmann et al., 2016). Thus, the decline in size diversity and the dominance of medium-size cities may reflect a decrease in the stability of urban systems. To quantitatively measure the stability changes in urban systems, the effective potential (EP) was introduced, as the most stable state of a system is the one with the minimum EP (Martín et al., 2015). The derivation shows that the EP value is positively correlated with  $b$  (Equation 10), thus the increasing trend of  $b$  values demonstrates that the stability of urban systems is weakening.

To further quantify the resilience alterations in urban systems, power spectrum analysis (Bak et al., 1987) was performed on the ordered power law phase. The results showed that all regions initially had “pink” power spectrums ( $\gamma < 0$ ) for the power law distributed urban areas, which then turned “blue” ( $\gamma > 0$ ) and became “bluer” over time (Figure 3f). With this “blue shift” tendency of the area power spectrum, the system autocorrelation function exhibits a possibility of approaching infinity (Equation 11e). As increased autocorrelation is an early warning signal of declining system resilience (Scheffer et al., 2009), the “blue shift” trend of urban areas may also indicate a loss of urban system resilience, meaning that urban systems will take longer time to recover from perturbations (Pascual & Guichard, 2005). In addition, the values of  $H_{urst}$  have also increased and exceeded 0.5 in most regions since 2014 (Figure 3g), suggesting that the driving processes behind these trends have begun to operate in a persistent mode (Mandelbrot & Van Ness, 1968); thus, the possible alterations of system functioning may continue or even become more severe in the future.

## 4.3. Mechanism Underlying Changes of Urban Systems

Economies of scale are a widely accepted driver of population agglomeration and city formation (Batty, 2013; Bettencourt & West, 2010; Brenner & Schmid, 2015). While it is difficult to distinguish quantitatively between the internal and external parts, the influence of the latter on a region can be indirectly reflected by the value of the region's globalization index (GI, Gygli et al., 2019), as the interconnectedness and interdependence between regions has been strengthened by globalization (Brady et al., 2007; Gu, 2019; Young et al., 2006). The rising GI

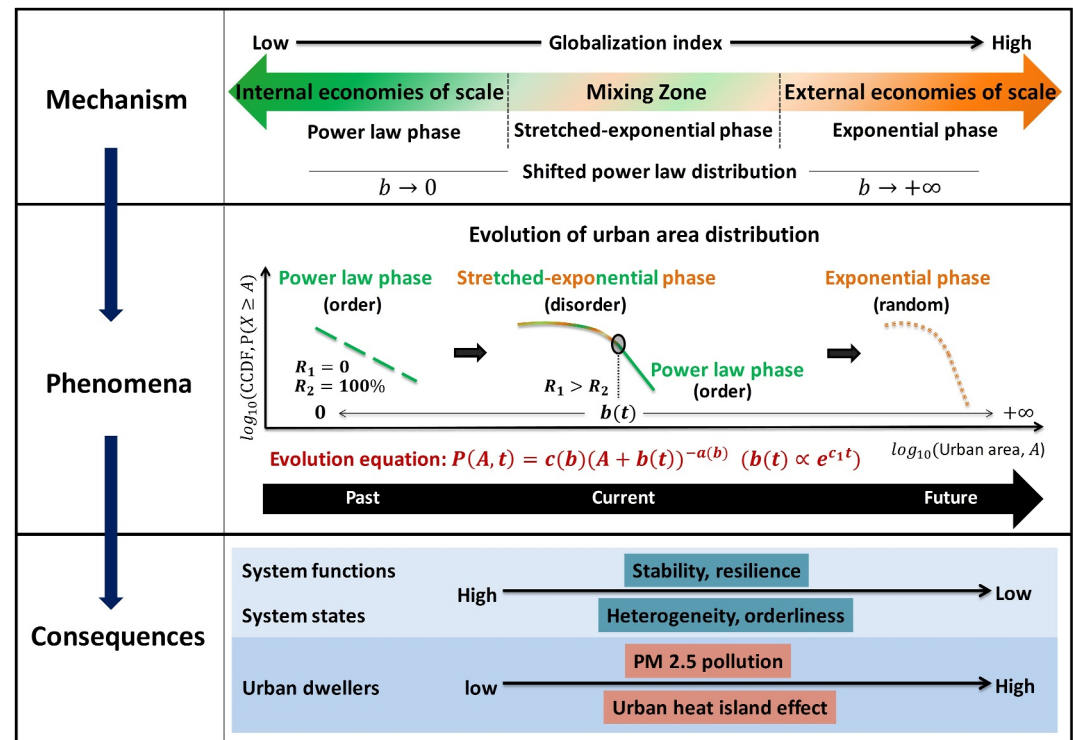


**Figure 4.** Evolutionary process of global urban land expansion: statistical characteristics (phenomena), underlying mechanisms, and impacts on urban systems and their inhabitants (consequences). **Phenomena:** Urban area distributions have shifted from the initial power law distribution (Phase I) to the current state where the stretched-exponential (Phase II) and power law phase coexist, and are likely to approach the exponential distribution (Phase III) in the future. **Mechanism:** The dominant driving force of urban systems changing from internal economies of scale to external economies of scale is the main reason for the shift of urban area distributions from power law to exponential distribution. **Consequences:** The urban area distribution shift is accompanied by a decrease in system stability and resilience and an increase in the exposure of urban dwellers to extreme heat events and air pollution.

values shown in Figure 3h demonstrate that the 14 study regions have become more closely interconnected over the past 29 years, thus intensifying the influence of external economies of scale on each region.

The shift coefficient  $b$ , which represents the evolutionary characteristics of urban systems, correlates positively with the GI values in all regions (Figure 3i), suggesting that the increased influence from external economies of scale may be one of the driving factors leading to the evolutionary characteristics of urban systems. The phase transition in the urban area distributions, characterized by the contraction of power law phase and the expansion of stretched-exponential phase, can be linked to the shift of the driving force from internal to external. This correspondence is particularly evident in China, where the urban area distribution in 1992 contained solely the power law phase, but the stretched-exponential phase overtook it and accounted for over 60% by 2020 (Figures 1 and 3e). Although China opened up to the outside since 1978, the degree of openness was low in (and before) 1992 (Figure 3h) and the interactions among cities within the country were also weak due to the underdeveloped transportation infrastructure and restrictions imposed by the “hukou” (urban residence permit) policy (Gu, 2019). Therefore, internal economies of scale (internal force) played a dominant role in 1992 and the urban areas followed the power law distribution. After joining the WTO in 2001, the influence of external economies of scale (external force) gradually intensified and thus the power law phase shrank, while the stretched-exponential phase appeared and expanded under the mixed effect of internal and external economies of scale. Since urban areas will approach an exponential distribution as  $b \rightarrow \infty$  while  $b$  and  $a$  are linearly correlated, we hypothesized that an exponential area distribution will emerge when external economies of scale play a dominant role. Based on these analyses, we proposed a new mechanism to explain the observed changes in the urban systems, as shown in Figure 4.

**Table 2**  
Value Variations of Distribution Function Coefficients, State Indicators and Power Spectrum Variables Between 1992 and 2020

Regions	Distribution function coefficients		State indicators			Power spectrum variables	
	<i>b</i>	<i>a</i>	CV	H	$R_2$	$\gamma$	$H_{urst}$
Global	24.18	0.58	-2.32	2.16	16.44%	0.38	0.19
EU	17.42	0.47	-1.72	1.65	5.97%	0.28	0.14
NA	21.19	0.31	-1.33	0.84	-4.85%	0.20	0.10
OA	8.04	0.44	-1.02	1.14	30.04%	0.33	0.16
AF	31.38	0.65	-2.46	1.75	28.53%	0.41	0.20
AS	20.85	0.51	-2.96	2.57	22.82%	0.31	0.16
SA	31.27	0.74	-2.15	1.98	-1.64%	0.47	0.24
USA	24.1	0.38	-1.21	0.80	4.78%	0.25	0.12
India	17.36	0.58	-1.76	1.93	50.70%	0.35	0.18
China	23.98	0.54	-2.25	2.76	61.60%	0.30	0.15
NZ	12.63	0.3	-0.63	1.14	39.91%	0.18	0.09
SZ	24.69	0.39	-2.38	2.14	62.72%	0.18	0.09
CZ	23.88	0.5	-0.50	2.49	41.75%	0.21	0.10
WZ	23.12	0.65	-0.66	2.38	55.63%	0.34	0.17

Note. Distribution function coefficients: shift coefficient (*b*) and scaling exponent (*a*); State indicators: coefficient of variation (CV), information entropy (H) and portion of the stretched-exponential phase ( $R_2$ ); Power spectrum variables: spectrum exponent ( $\gamma$ ) and Hurst exponent ( $H_{urst}$ ). EU: Europe; NA: North America; OA: Oceania; AF: Africa; AS: Asia; SA: South America; NZ, SZ, CZ and WZ are the Northeast, Southeast, Central and Western economic zone of China, respectively.

#### 4.4. Implications and Limitations

##### 4.4.1. More Severe and Persistent in Developing Regions

Despite the consistency in the overall trends, regional differences still exist, especially between developed and developing regions, as shown by the different values of the distribution function coefficients and system state indicators across regions and over the years (Figure 3). In general, the values of these quantities are larger in developed regions, especially before 2014 (Figure 3), due to the fact that developed regions completed urbanization before 1992, while developing regions are still in the process of urbanization. However, the magnitude of the change in values between 1992 and 2020 is more dramatic in developing regions (Table 2), indicating that the degree to which the urban system state and functions have changed differs among the study regions and tends to be greater and more persistent in developing regions (see Text S5 in Supporting Information S1 for a detailed discussion).

##### 4.4.2. Importance of Medium-Size Cities in Mitigating UHI and PM2.5 Pollution

UHI and PM2.5 pollution are two environmental problems associated with urban land expansion that can directly affect the health of urban dwellers (Southerland et al., 2022; Tuholske et al., 2021). The intensity of UHI has been found to be positively correlated with urban area and the relationship could be described by a sigmoid function (Figure 5a) (Zhou et al., 2013), where we observed the fastest growth in UHI intensity in cities with an area between  $10^1$  and  $10^2$  km<sup>2</sup> (i.e., the medium-size cities we defined). As the dominant city type in urban systems has shifted from small-to medium-size cities, the current path of land urbanization tends to exacerbate the UHI. By including UHI data (Tuholske et al., 2021) in our analysis, we found a positive correlation between the total exposure of urban populations and the

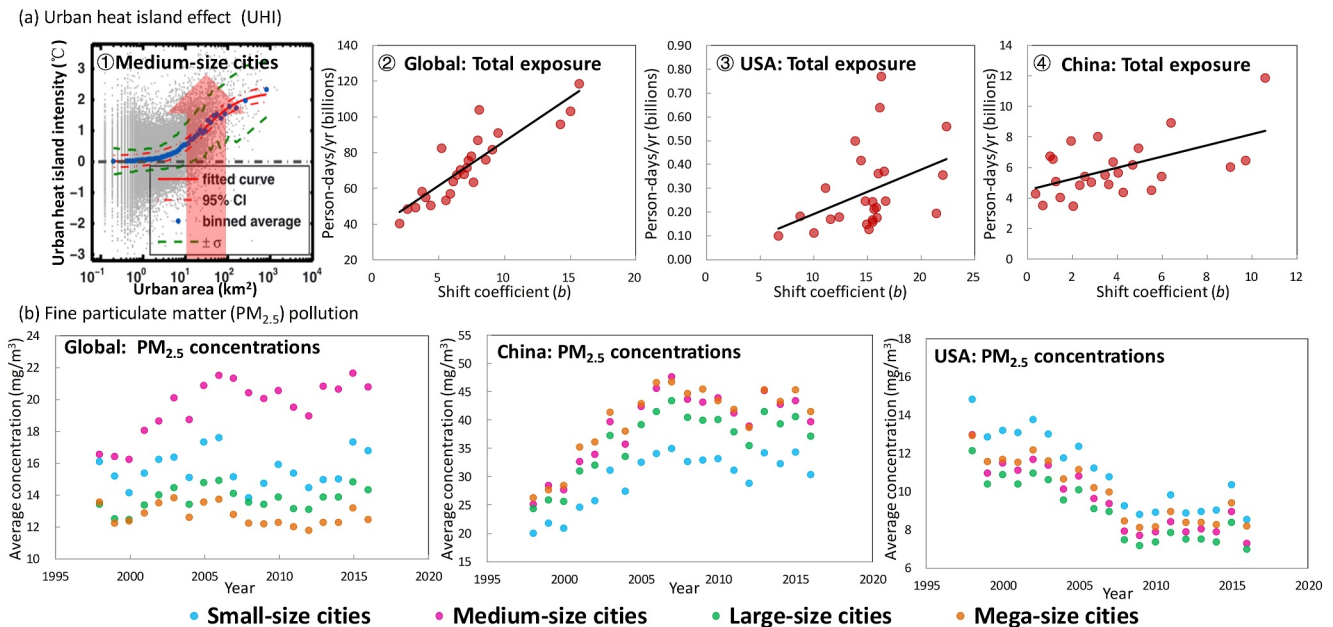


**Figure 5.** Impacts of urban system alterations on urban dwellers. (a) Urban heat island effect (UHI): ①: Relationship between the UHI intensity and urban land area (Zhou et al., 2013); ②-④: Positive correlation between the total exposure of urban populations to extreme heat and the shift coefficient (*b*). (b) Fine particulate matter (PM2.5) pollution: average PM2.5 concentrations for each city type.

shift coefficient  $b$  for all study regions (Figure 5a), indicating that as the urban systems evolve, the risk of their dwellers being exposed to extreme heat events tends to increase. For PM<sub>2.5</sub> pollution (CIESIN, 2021), we found that the highest PM<sub>2.5</sub> concentrations globally and in developing regions occur in the medium-size cities, while in developed regions they occur in the small-size ones (Figure 5b). Therefore, the shift in the dominant city type from small-to medium-size cities could exacerbate the PM<sub>2.5</sub> pollution in developing regions but mitigate it in developed regions. These results provide preliminary indications of the importance of medium-size cities in mitigating UHI and PM<sub>2.5</sub> pollution.

#### 4.4.3. Possible Future Trajectory of Land Urbanization

The evolution equation of the urban area distribution could provide an insight into the possible trajectory of land urbanization in the future. According to the mathematical properties of this equation, the urban area distribution will approach an exponential or even a uniform distribution as  $b$  increases to infinity. Based on the equation, we calculated that the power law phase of the urban area distribution would disappear by 2100 in most of the study regions (Table S3 in Supporting Information S1). Does this mean that the urban area distribution of global urban systems would shift to these two statistical distributions at that time if the current scenario of land urbanization continues? Previous studies have shown that the exponential distribution represents a random state (Cox, 1955), while the uniform distribution is like a thermodynamic equilibrium-like state where cities of all sizes occur with equal probability (Prigogine & Lefever, 1973). What would be the consequences for urban systems and urban residents if the distribution shift were to occur? Although more research is needed to answer these questions, we pose them to provoke a rethinking of current land urbanization practices in order to ensure a sustainable future for humanity.

#### 4.4.4. Limitations

How a city is defined can affect the results of statistical analyses of urban land area, widely known as the modifiable area unit problem (Barthelemy, 2019; Bettencourt, 2021). As there is no consensus on the definition of cities in urban science, different studies often use different delineations of the spatial extent of cities depending on their research context and scope (Dong et al., 2024). It is necessary to reemphasize that the cities discussed in this work refers to urban regions associated with high-intensity human settlement and socio-economic activities identified based on nighttime lights (Zhao et al., 2021). Besides, the data resolution may also have an impact on the statistical results, but there are currently no urban extent data with a resolution higher than 1 km based on nighttime lights. Although urban extent data based on other satellites have higher resolution, they are not suitable for analyzing the impact of data resolution on our results because of the different definitions of cities (Potere et al., 2009). These effects mentioned above can be investigated in the future when a harmonized definition of city and suitable data are available.

While our primary focus is on the land dimension of urban dynamics, the evolution of urban systems is inextricably linked to social, economic and political factors that influence the land development and organization practices (Solecki et al., 2013). Future research should aim to unify these dimensions of urbanization to advance urban science with predictive theories and models, thereby advancing an ambitious urban sustainable development agenda. For example, since the urban land follows the shifted power law distribution, if the population size is related to urban land area in a power function (Text S6, Equation S12 in Supporting Information S1), as previous studies have shown (Bettencourt, 2013; Bettencourt & West, 2010; Bettencourt & Zünd, 2020), then population size will have a shifted power law form distribution (Equations S13a and S13b in Supporting Information S1) instead of a power law distribution. This may help to explain the inconsistencies in the population size distribution and its driving mechanism (Arshad et al., 2018). Our analysis of urban system changes on urban dwellers only considered UHI and PM<sub>2.5</sub>, and was also preliminary. In future studies, we will integrate multi-source environmental data and human health data related to urban land expansion to quantify the effects of urban system changes to provide a more comprehensive and in-depth understanding of urbanization.

## 5. Conclusions

We report a cross-scale convergent evolution of urban land expansion over a 29 year period in 14 countries and regions with different political, economic, cultural and geographic conditions. We find that as urban area distributions deviate from the initial power law distributions, the urban systems gradually become dominated by the

medium-size cities and become more homogeneous and disordered in state, leading to a decline in system stability and resilience. The driving mechanism underlying the changes of urban systems can be linked to the increased influence of external economies of scale associated with globalization. The exposure of urban populations to extreme heat events and air pollution has also increased during this process, but effective control of the urban heat island effect and PM<sub>2.5</sub> concentrations in medium-size cities, especially those in developing regions, would mitigate these problems. Our findings highlight the need to rethink current land urbanization practices to ensure a sustainable future for humanity.

### Conflict of Interest

The authors declare no conflicts of interest relevant to this study.

### Data Availability Statement

The data on which this paper is based include the global annual urban extent data set, the globalization index (GI) data, the global high resolution daily extreme urban heat exposure data set (UHE-Daily, 1983–2016) and the annual PM<sub>2.5</sub> concentrations for countries and urban areas data set (1998–2016), available in Zhao et al. (2021), Gygli et al. (2019), Tuholske et al. (2021) and CIESIN (2021), respectively.

### Acknowledgments

This research is supported by the Center for Balance Architecture of Zhejiang University (Project No: K Heng 20203512-02B, Index and planning methods of resilient cities).

### References

- Acuto, M., Parnell, S., & Seto, K. C. (2018). Building a global urban science. *Nature Sustainability*, *1*(1), 2–4. <https://doi.org/10.1038/s41893-017-0013-9>
- Angel, S. (2023). Urban expansion: Theory, evidence and practice. *Building Cities*, *4*(1), 124–138. <https://doi.org/10.5334/bc.348>
- Arshad, S., Hu, S., & Ashraf, B. N. (2018). Zipf's law and city size distribution: A survey of the literature and future research agenda. *Physica A: Statistical Mechanics & Its Applications*, *S0378437117310130*.
- Bak, P., Tang, C., & Wiesenfeld, K. (1987). Self-organized criticality: An explanation of the  $1/f$  noise. *Physical Review Letters*, *59*(4), 381–384. <https://doi.org/10.1103/physrevlett.59.381>
- Barthelemy, M. (2019). The statistical physics of cities. *Nature Reviews Physics*, *1*(6), 406–415. <https://doi.org/10.1038/s42254-019-0054-2>
- Batty, M. (2013). A theory of city size. *Science*, *340*(6139), 1418–1419. <https://doi.org/10.1126/science.1239870>
- Batty, M., & Ferguson, P. (2011). Defining city size. *Environment and Planning B: Planning and Design*, *38*(5), 753–756. <https://doi.org/10.1068/b3805ed>
- Bettencourt, L., & West, G. (2010). A unified theory of urban living. *Nature*, *467*(7318), 912–913. <https://doi.org/10.1038/467912a>
- Bettencourt, L. M. (2013). The origins of scaling in cities. *Science*, *340*(6139), 1438–1441. <https://doi.org/10.1126/science.1235823>
- Bettencourt, L. M. (2021). *Introduction to urban science: Evidence and theory of cities as complex systems*. MIT Press.
- Bettencourt, L. M., & Zünd, D. (2020). Demography and the emergence of universal patterns in urban systems. *Nature Communications*, *11*(1), 4584. <https://doi.org/10.1038/s41467-020-18205-1>
- Birkmann, J., Welle, T., Solecki, W., Lwasa, S., & Garschagen, M. (2016). Boost resilience of small and mid-sized cities. *Nature*, *537*(7622), 605–608. <https://doi.org/10.1038/537605a>
- Bowley, R. M., & Sánchez, M. (1999). *Introductory statistical mechanics*. Clarendon.
- Brady, D., Beckfield, J., & Zhao, W. (2007). The consequences of economic globalization for affluent democracies. *Annual Review of Sociology*, *33*(1), 313–334. <https://doi.org/10.1146/annurev.soc.33.040406.131636>
- Brenner, N., & Schmid, C. (2015). Towards a new epistemology of the urban? *Next City*, *19*(2–3), 151–182. <https://doi.org/10.1080/13604813.2015.1014712>
- Center for International Earth Science Information Network (CIESIN), Columbia University. (2021). Annual PM<sub>2.5</sub> concentrations for countries and urban areas, 1998–2016. Palisades, NY: NASA socioeconomic data and applications center (SEDAC) [Dataset]. *EARTHDATA*. Retrieved from <https://earthdata.nasa.gov/data/catalog/sedac-ciesin-sedac-sdei-apm25-urban-1.00>
- Chen, J., Liu, T., Huang, Z., & Su, G. (2018). Probability distribution function of complex systems. *International Journal of Modern Physics B*, *32*(03), 1850022. <https://doi.org/10.1142/s0217979218500224>
- Cox, D. R. (1955). A use of complex probabilities in the theory of stochastic processes. *Mathematical Proceedings of the Cambridge Philosophical Society*, *51*(2), 313–319. Cambridge University Press. <https://doi.org/10.1017/s0305004100030231>
- Dong, L., Duarte, F., Duranton, G., Santi, P., Barthelemy, M., Batty, M., et al. (2024). Defining a city—Delineating urban areas using cell-phone data. *Nature Cities*, *1*(2), 117–125. <https://doi.org/10.1038/s44284-023-00019-z>
- Elmqvist, T., Folke, C., Nyström, M., Peterson, G., Bengtsson, J., Walker, B., & Norberg, J. (2003). Response diversity, ecosystem change, and resilience. *Frontiers in Ecology and the Environment*, *1*(9), 488–494. <https://doi.org/10.2307/3868116>
- Fan, J., Meng, J., Ludescher, J., Chen, X., Ashkenazy, Y., Jürgen, K., et al. (2021). Statistical physics approaches to the complex earth system. *Physics Reports*, *896*, 1–84. <https://doi.org/10.1016/j.physrep.2020.09.005>
- Gu, C. (2019). Urbanization: Processes and driving forces. *Science China Earth Sciences*, *62*(9), 1351–1360. <https://doi.org/10.1007/s11430-018-9359-y>
- Gygli, S., Haelg, F., Potrafke, N., & Sturm, J. E. (2019). The KOF globalisation index—revisited. *The Review of International Organizations*, *14*(3), 543–574. [Dataset]. KOF. <https://doi.org/10.1007/s11558-019-09344->
- Habitat, U. N. (2022). *World cities report 2022: Envisaging the future of cities*. United Nations Research Institute for Social Development.
- Halley, J. M. (1996). Ecology, evolution and  $1/f$ -noise. *Trends in Ecology and Evolution*, *11*(1), 33–37. [https://doi.org/10.1016/0169-5347\(96\)81067-6](https://doi.org/10.1016/0169-5347(96)81067-6)
- He, C., Zhang, Y., Schneider, A., Chen, R., Zhang, Y., Ma, W., et al. (2022). The inequality labor loss risk from future urban warming and adaptation strategies. *Nature Communications*, *13*(1), 3847. <https://doi.org/10.1038/s41467-022-31145-2>

- Holovatch, Y., Kenna, R., & Thurner, S. (2017). Complex systems: Physics beyond physics. *European Journal of Physics*, 38(2), 023002. <https://doi.org/10.1088/1361-6404/aa5a87>
- Hu, S., Yang, Z., Torres, S., Wang, Z., & Li, L. (2023). Size distributions reveal regime transition of lake systems under different dominant driving forces. *Water Resources Research*, 59(8), e2022WR034024. <https://doi.org/10.1029/2022wr034024>
- Jacobs, J. (1961). *The death and life of great American cities*. Random House.
- Kubo, R., Toda, M., & Hashitsume, N. (2012). *Statistical physics II: Nonequilibrium statistical mechanics* (Vol. 31). Springer Science and Business Media.
- Laurance, W. F., & Engert, J. (2022). Sprawling cities are rapidly encroaching on Earth's biodiversity. *Proceedings of the National Academy of Sciences*, 119(16), e2202244119. <https://doi.org/10.1073/pnas.2202244119>
- Levin, N., Kyba, C. C., Zhang, Q., de Miguel, A. S., Román, M. O., Li, X., et al. (2020). Remote sensing of night lights: A review and an outlook for the future. *Remote Sensing of Environment*, 237, 111443. <https://doi.org/10.1016/j.rse.2019.111443>
- Liang, W., & Yang, M. (2019). Urbanization, economic growth and environmental pollution: Evidence from China. *Sustainable Computing: Informatics and Systems*, 21, 1–9. <https://doi.org/10.1016/j.suscom.2018.11.007>
- Loreau, M., & De Mazancourt, C. (2013). Biodiversity and ecosystem stability: A synthesis of underlying mechanisms. *Ecology Letters*, 16(1), 106–115. <https://doi.org/10.1111/ele.12073>
- Mandelbrot, B. (1953). An informational theory of the statistical structure of language. *Communication Theory*, 84, 486–502.
- Mandelbrot, B. B., & Van Ness, J. W. (1968). Fractional Brownian motions, fractional noises and applications. *SIAM Review*, 10(4), 422–437. <https://doi.org/10.1137/1010093>
- Mao, A. H., Sun, F. H., & Lin, W. J. (2008). Comparative study on urbanizations of developed and developing countries. *Human Geography*, 23, 41–45.
- Meyfroidt, P., De Bremond, A., Ryan, C. M., Archer, E., Aspinall, R., Chhabra, A., et al. (2022). Ten facts about land systems for sustainability. *Proceedings of the National Academy of Sciences*, 119(7), e2109217118. <https://doi.org/10.1073/pnas.2109217118>
- Michaelides, E. E. (2008). Entropy, order and disorder. *The Open Thermodynamics Journal*, 2(1), 7–11. <https://doi.org/10.2174/1874396x00802010007>
- Newman, M. E. (2005). Power laws, Pareto distributions and Zipf's law. *Contemporary Physics*, 46(5), 323–351. <https://doi.org/10.1080/00107510500052444>
- Ouyang, Z., Sciusco, P., Jiao, T., Feron, S., Lei, C., Li, F., et al. (2022). Albedo changes caused by future urbanization contribute to global warming. *Nature Communications*, 13(1), 3800. <https://doi.org/10.1038/s41467-022-31558-z>
- Pascual, M., & Guichard, F. (2005). Criticality and disturbance in spatial ecological systems. *Trends in Ecology and Evolution*, 20(2), 88–95. <https://doi.org/10.1016/j.tree.2004.11.012>
- Potere, D., Schneider, A., Angel, S., & Civco, D. L. (2009). Mapping urban areas on a global scale: Which of the eight maps now available is more accurate? *International Journal of Remote Sensing*, 30(24), 6531–6558. <https://doi.org/10.1080/01431160903121134>
- Prigogine, I., & Lefever, R. (1973). *Theory of dissipative structures in Synergetics: Cooperative phenomena in multi-component systems*. Springer.
- Rozenfeld, H. D., Rybski, D., Gabaix, X., & Makse, H. A. (2011). The area and population of cities: New insights from a different perspective on cities. *The American Economic Review*, 101(5), 2205–2225. <https://doi.org/10.1257/aer.101.5.2205>
- Scheffer, M., Bascompte, J., Brock, W. A., Brovkin, V., Carpenter, S. R., Dakos, V., et al. (2009). Early-warning signals for critical transitions. *Nature*, 461(7260), 53–59. <https://doi.org/10.1038/nature08227>
- Seto, K. C., & Fragkias, M. (2005). Quantifying spatiotemporal patterns of urban land-use change in four cities of China with time series landscape metrics. *Landscape Ecology*, 20(7), 871–888. <https://doi.org/10.1007/s10980-005-5238-8>
- Shi, K., Wu, Y., Liu, S., Chen, Z., Huang, C., & Cui, Y. (2023). Mapping and evaluating global urban entities (2000–2020): A novel perspective to delineate urban entities based on consistent nighttime light data. *GIScience and Remote Sensing*, 60(1), 2161199. <https://doi.org/10.1080/15481603.2022.2161199>
- Solecki, W., Seto, K. C., & Marcotullio, P. J. (2013). It's time for an urbanization science. *Environment: Science and Policy for Sustainable Development*, 55(1), 12–17. <https://doi.org/10.1080/00139157.2013.748387>
- Sornette, D. (2007). Probability distributions in complex systems. *arXiv preprint arXiv:0707.2194*.
- Southerland, V. A., Brauer, M., Moheg, A., Hammer, M. S., Van Donkelaar, A., Martin, R. V., et al. (2022). Global urban temporal trends in fine particulate matter (PM<sub>2.5</sub>) and attributable health burdens: Estimates from global datasets. *The Lancet Planetary Health*, 6(2), e139–e146. [https://doi.org/10.1016/s2542-5196\(21\)00350-8](https://doi.org/10.1016/s2542-5196(21)00350-8)
- Tuholske, C., Caylor, K., Funk, C., Verdin, A., Sweeney, S., Grace, K., et al. (2021). Global urban population exposure to extreme heat. *Proceedings of the National Academy of Sciences*, 118(41), e2024792118. [Dataset]. EARTHDATA. <https://doi.org/10.1073/pnas.2024792118>
- Villa Martín, P., Bonachela, J. A., Levin, S. A., & Muñoz, M. A. (2015). Eluding catastrophic shifts. *Proceedings of the National Academy of Sciences*, 112(15), E1828–E1836. <https://doi.org/10.1073/pnas.1414708112>
- Villegas, P., Gili, T., & Caldarelli, G. (2021). Emergent spatial patterns of coexistence in species-rich plant communities. *Physical Review*, 104(3), 034305. <https://doi.org/10.1103/physreve.104.034305>
- Wornell, G. W. (1993). Wavelet-based representations for the 1/f family of fractal processes. *Proceedings of the IEEE*, 81(10), 1428–1450. <https://doi.org/10.1109/5.241506>
- Young, O. R., Berkhout, F., Gallopin, G. C., Janssen, M. A., Ostrom, E., & Van der Leeuw, S. (2006). The globalization of socio-ecological systems: An agenda for scientific research. *Global Environmental Change*, 16(3), 304–316. <https://doi.org/10.1016/j.gloenvcha.2006.03.004>
- Zaccone, A. (2020). Relaxation and vibrational properties in metal alloys and other disordered systems. *Journal of Physics: Condensed Matter*, 32(20), 203001. <https://doi.org/10.1088/1361-648x/ab6e41>
- Zhao, M., Cheng, C., Zhou, Y., Li, X., Shen, S., & Song, C. (2021). A global dataset of annual urban extents (1992–2020) from harmonized nighttime lights. *Earth System Science Data Discussions*, 2021, 1–25. [Dataset]. figshare [https://figshare.com/articles/dataset/A\\_global\\_dataset\\_of\\_annual\\_urban\\_extents\\_1992-2020\\_from\\_harmonized\\_nighttime\\_lights/16602224/1](https://figshare.com/articles/dataset/A_global_dataset_of_annual_urban_extents_1992-2020_from_harmonized_nighttime_lights/16602224/1)
- Zhou, B., Rybski, D., & Kropp, J. P. (2013). On the statistics of urban heat island intensity. *Geophysical Research Letters*, 40(20), 5486–5491. <https://doi.org/10.1002/2013gl057320>

## References From the Supporting Information

- Chowdhry, B., & Goyal, A. (2000). Understanding the financial crisis in Asia. *Pacific-Basin Finance Journal*, 8(2), 135–152. [https://doi.org/10.1016/s0927-538x\(00\)00011-1](https://doi.org/10.1016/s0927-538x(00)00011-1)

- Foo, J., & Witkowska, D. (2017). A comparison of global financial market recovery after the 2008 global financial crisis. *Folia Oeconomica Stetinensia*, *17*(1), 109–128. <https://doi.org/10.1515/fofi-2017-0009>
- Kasdin, N. J. (1995). Discrete simulation of colored noise and stochastic processes and 1/f power law noise generation. *Proceedings of the IEEE*, *83*(5), 802–827. <https://doi.org/10.1109/5.381848>
- Lu, D., Xu, X., Tian, H., Moran, E., Zhao, M., & Running, S. (2010). The effects of urbanization on net primary productivity in southeastern China. *Environmental Management*, *46*(3), 404–410. <https://doi.org/10.1007/s00267-010-9542-y>
- Lu, Z., & Deng, X. (2011). *China's western development strategy: Policies, effects and prospects*. MPRA Paper.
- Ritchie, H., & Roser, M. (2018). Urbanization. Published online at OurWorldInData.org. Retrieved from <https://ourworldindata.org/urbanization>. Accessed in 10/02/2023.
- Sulemana, I., Nketiah-Amponsah, E., Codjoe, E. A., & Andoh, J. A. N. (2019). Urbanization and income inequality in sub-Saharan Africa. *Sustainable Cities and Society*, *48*, 101544. <https://doi.org/10.1016/j.scs.2019.101544>
- Vasseur, D. A., & Yodzis, P. (2004). The color of environmental noise. *Ecology*, *85*(4), 1146–1152. <https://doi.org/10.1890/02-3122>